PHYSOR 2004 - The Physics of Fuel Cycles and Advanced Nuclear Systems: Global Developements
Chicago, Illinois, April 25-29, 2004, on CD-ROM, American Nuclear Society, Lagrange Park, IL. (2004)

Creation of a Simplified Benchmark Model for the Neptunium Sphere Experiment

Russell D. Mosteller[*1], David J. Loaiza,[1]and Rene G. Sanchez[1]
[1]*Los Alamos National Laboratory, P. O. Box 1663, Los Alamos, NM 87545 USA*

A simplified benchmark model has been constructed for a critical experiment in which a 6-kg sphere of ^{237}Np was surrounded by nested hemishells of highly enriched uranium. The simplified benchmark model retains all of the neutronically important aspects of the detailed model of the experiment and substantially reduces the computer resources required for the calculation. However, both the detailed and simplified benchmark models underpredict k_{eff} by more than 1% Δk. This discrepancy supports the suspicion that better cross sections are needed for ^{237}Np.

KEYWORDS: Neptunium, Criticality, Benchmarks, MCNP

1. Introduction

Although neptunium is produced in significant amounts by nuclear power reactors, its critical mass is not well known. In addition, sizeable uncertainties exist for its cross sections. As an important step toward resolution of these issues, a critical experiment was conducted in 2002 at the Los Alamos Critical Experiments Facility (LACEF). In the experiment, a 6-kg sphere of ^{237}Np was surrounded by nested hemispherical shells of highly enriched uranium (HEU). [1-4] The HEU shells were required in order to reach a critical condition.

Subsequently, a detailed model of the experiment was developed [5]. This model faithfully reproduces the components of the experiment, but it is geometrically complex. Furthermore, the isotopics analysis upon which that model is based omits nearly 1% of the mass of the sphere. The objective of the study reported herein was to produce a simplified benchmark model that removes the geometric complexity but retains all the important aspects of its neutronic behavior. As part of that process, the reactivity impact of the missing mass has been quantified.

2. Description of Experiment

The experiment was performed on the Planet vertical assembly at LACEF. The Planet assembly has two primary components: a stationary platform that supports a stainless-steel membrane to hold the upper portion of the experimental assembly in place, and a vertical drive that lifts the lower portion of the assembly upward. In this particular experiment, the upper portion of the assembly contained 14 hemispherical HEU shells, while the lower portion contained 15 hemispherical HEU shells and the neptunium sphere. An aluminum spacer was placed on top of the lower HEU shells to prevent a configuration that would exceed operating limits. The neptunium sphere was enclosed in a tungsten shell to reduce the radiological hazard, and that shell, in turn, was coated with two

* Corresponding author, Tel. 505-665-4879, FAX 505-665-3046, E-mail: mosteller@lanl.gov

separate layers of nickel cladding. A slightly idealized schematic of the experimental configuration is shown in Figure 1.

3. Benchmark Simplifications

Three sequential steps were taken to produce a simplified benchmark model. First, the impact of the missing mass was assessed. Next, a set of geometric approximations was introduced, and the reactivity impact of those approximations was quantified. Finally, a series of material simplifications was incorporated, and the reactivity impact of those approximations was determined.

All of the calculations were performed with the MCNP5™ Monte Carlo code [6] and a combination of the ACTI [7] and ENDF66 [8] nuclear data libraries that corresponds to the final version of ENDF/B-VI [9]. Each calculation employed 650 generations of 10,000 neutrons each, and the results from the first 50 generations were discarded. Consequently, the results from each case are based on 6,000,000 active neutron histories.

Previous simplifications were retained at each step in the process. Consequently, the standard deviations associated with the calculations are not compounded, and the results from any step can be compared directly with those from any other step.

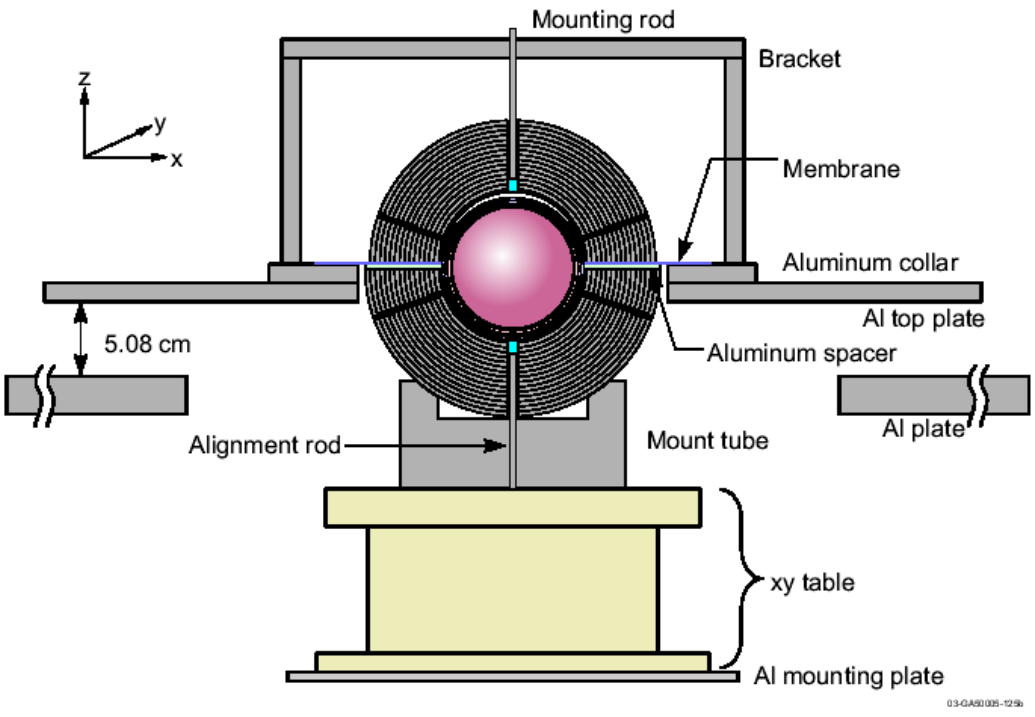

Fig. 1 Schematic of the Experiment.

MCNP is a trademark of the Regents of the University of California, Los Alamos National Laboratory

3.1 Missing Mass

The composition of the sphere was determined from a chemical assay of the sprue. Unfortunately, that sample did not dissolve completely, leaving 0.946 wt.% of the mass of the sphere unaccounted for. The "missing" mass could be any of a number of components or some combination of them. The sphere was cast in a graphite mold with a lining of erbia power. In addition, iron is a common impurity from the casting process, and it has been reported that europium is often a contaminant in neptunium refined from spent reactor fuel [10]. Alternatively, it is possible that the undissolved material was very similar to the dissolved portion and was effectively pure neptunium.

MCNP5 calculations were performed to assess the reactivity impact of these alternatives, and the results from those calculations are presented in Table 1. It is clear that the impact of the missing mass is quite small, irrespective of its actual composition. Based on the results from that table, representing the missing mass as void, with an associated uncertainty of ± 0.0012 Δk, appears to be an adequate approximation. The benchmark value of k_{eff} for the detailed model of the experiment previously was determined to be 1.0026 ± 0.0034 [4], based on the measured excess reactivity and the uncertainties associated with the experiment. When the additional uncertainty for the missing mass is folded into that value, the final benchmark value of k_{eff} for the detailed model becomes 1.0026 ± 0.0036.

3.2 Geometric Simplifications

The geometric simplifications that were made and their corresponding impact on reactivity are summarized in Table 2. Some structural components and the aluminum spacer were retained because their removal produces a reactivity change that is unacceptably large. Removal of the spacer, for example, increases reactivity by approximately 1% Δk. Similarly, complete removal of the bridge base, collar, and platform produces an unacceptable reduction in reactivity. Instead, they have been combined into a single ring that approximately conserves the cumulative reactivity contribution from all three.

Table 1 Reactivity Effect of Missing Mass.

Missing mass represented as	Δk	Fission Fraction	
		^{237}Np	^{235}U
Void	—	0.1264	0.8570
Carbon	-0.0005 ± 0.0004	0.1257	0.8577
Iron	-0.0002 ± 0.0004	0.1257	0.8576
Europium	-0.0011 ± 0.0004	0.1258	0.8576
Erbium*	0.0004 ± 0.0004	0.1259	0.8574
^{237}Np	0.0012 ± 0.0004	0.1278	0.8556

* Only ^{166E}Er and ^{167}Er present

Table 2 Reactivity Impact of Geometric Simplifications.

Change	Δk
Remove bridge	-0.0001 ± 0.0003
Remove mounting plate	-0.0007 ± 0.0003
Remove aluminum support plate	-0.0002 ± 0.0003
Remove X-Y alignment table	-0.0018 ± 0.0003
Remove empty holes in HEU hemishells	0.0002 ± 0.0003
Remove aluminum stems	-0.0010 ± 0.0003
Simplify aluminum mounting tube	0.0001 ± 0.0003
Remove membrane	0.0014 ± 0.0003
Convert bridge base, collar, and top plate into cylindrical ring	0.0006 ± 0.0003
Cumulative change	-0.0015 ± 0.0003

The simplifications that produce the largest reactivity changes are the removal of the X-Y alignment table, the aluminum stems, and the steel membrane. However, none of the reactivity changes for any individual simplification exceeds ± 0.0020 Δk, and the net effect of all of them is only -0.0015 ± 0.0003 Δk.

3.3 Material Simplifications

The detailed model of the experiment [5] explicitly represents each HEU hemishell with its own dimensions and mass. It also explicitly represents the gaps between the hemishells, as well as the gaps between the neptunium sphere and each layer of its cladding.

The density of the HEU hemishells first was changed to a uniform average value, although their thicknesses still varied from one hemishell to another. Subsequently, the hemishells were homogenized with the gaps between them to produce a single homogeneous hemisphere for the lower hemishells and another such hemisphere for the upper hemishells. Next, the aluminum liners for the innermost hemishells were homogenized with the gaps around them to create homogeneous regions that fit snugly against the homogenized HEU hemispheres. The homogenization of the lower aluminum liner also included the gap between it and the nickel cladding of the sphere. However, the gap between the aluminum liner for the upper HEU hemishells and the nickel cladding was retained in the benchmark model. It is relatively large and irregularly shaped, and homogenizing it with that aluminum liner would have distorted the distribution of the aluminum without reducing the geometric complexity of the model in any meaningful way. Finally, the tungsten cladding was homogenized with the gap between it and the neptunium sphere, and the two layers of nickel were homogenized with the gaps they enclose.

The reactivity changes from these simplifications are summarized in Table 3. Homogenizing the HEU hemishells with the gaps they enclose increases reactivity slightly, which is not surprising

because, on average, it moves the uranium slightly inward toward the neptunium sphere. The impact of the other changes is much smaller, but in the aggregate they partially offset the effect of homogenizing the HEU hemishells. The net effect is a reactivity change of only 0.0008 ± 0.0004 Δk.

3.4 Cumulative Effect of Simplifications

The results from Tables 2 and 3 can be combined to produce the final bias for the simplified benchmark model, as shown in Table 4. From section 3.1, the benchmark value of k_{eff} for the detailed model is 1.0026 ± 0.0036. Based on the cumulative reactivity impact of the simplifications, the benchmark value of k_{eff} for the simplified benchmark model therefore is 1.0019 ± 0.0036.

4. Calculated Results for the Detailed and Simplified Benchmark Models

After the simplified benchmark model had been determined, the MCNP input file was revised to make it as simple as possible while retaining complete consistency with the specifications for the simplified benchmark model. The results from that model are compared with those from the detailed model in Table 5. The comparison clearly demonstrates the equivalence of the two representations. Furthermore, the simplified benchmark consumes less than 40% as much CPU time as the detailed model. A schematic of the simplified benchmark model is shown in Figure 2, and a detailed set of specifications is provided in the Appendix.

Table 3 Reactivity Impact of Material Simplifications.

Change	Δk
Average density for all HEU hemishells	-0.0001 ± 0.0003
Homogenize HEU hemishells with enclosed gaps	0.0016 ± 0.0003
Homogenize aluminum liners with gaps	-0.0002 ± 0.0003
Homogenize tungsten and nickel cladding with enclosed gaps	-0.0005 ± 0.0004
Cumulative change	0.0008 ± 0.0004

Table 4 Cumulative Reactivity Impact of Simplifications.

Change	Δk
Geometric simplifications	-0.0015 ± 0.0003
Material Simplifications	0.0008 ± 0.0004
Cumulative change	-0.0007 ± 0.0004

Table 5 Comparison of Results from Detailed and Simplified Benchmark Models.

Parameter		Model	
		Detailed	Simplified Benchmark
k_{eff}		0.9896 ± 0.0002	0.9889 ± 0.0002
Fission Distribution, by Energy	Fast	0.9476	0.9478
	Intermediate	0.0524	0.0522
	Thermal	0.0	0.0
Fission Fraction, by Material	Np	0.1251	0.1255
	^{235}U	0.8584	0.8580
Average Energy of Neutrons Causing Fission (MeV)		1.516	1.519
Average Number of Neutrons Produced per Fission		2.636	2.637
Execution Time (CPU Minutes)*		74.25	27.50

*Calculations were performed on an 800 MHz PC running Windows 2000 Professional

As Table 5 indicates, the calculated values for k_{eff} for the detailed and benchmark models are 0.9896 ± 0.0002 and 0.9889 ± 0.0002, respectively. Consequently, the magnitude of the difference between the calculated and benchmark values for k_{eff} is more than 1% Δk, and it also is more than four times the the standard deviation associated with the benchmark value. That discrepancy supports the suspicion that better cross sections are needed for ^{237}Np.

5. Summary and Conclusions

A simplified benchmark model has been constructed for the Np sphere experiment. The model allows for the 0.946 wt.% of the mass of the sphere that is unaccounted for, and it has simplified representations for both the geometry of the experiment and the materials that comprise it. Furthermore, it retains all of the important neutronic aspects of the experiment, and it substantially reduces the computer resources required for the calculation.

The calculated results for both the detailed and simplified benchmark models underpredict k_{eff} by more than 1% Δk. This discrepancy supports the suspicion that better cross sections are needed for ^{237}Np.

Acknowledgments

This research was performed at Los Alamos National Laboratory under the auspices of contract W-7405-ENG-36 with the U. S. Department of Energy.

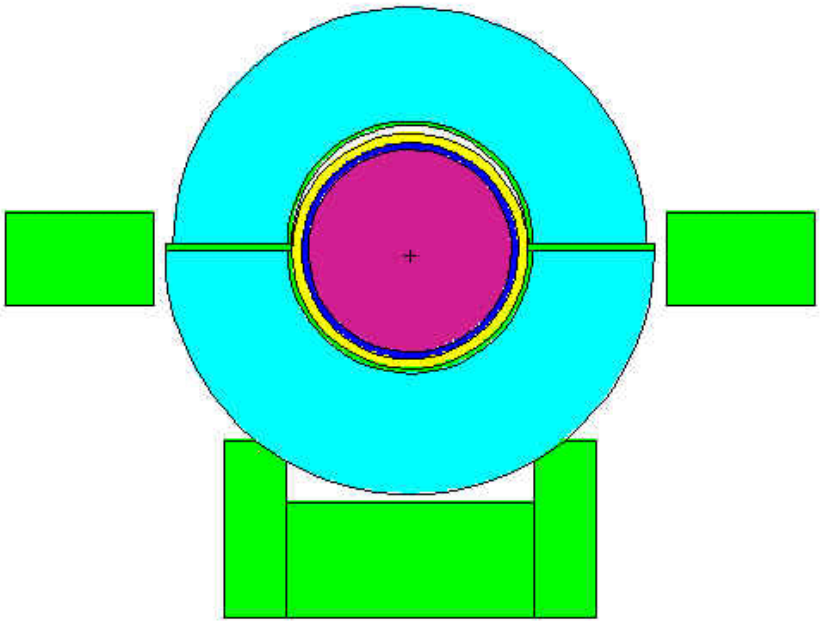

Fig. 2 Two-Dimensional Schematic of the Simplified Benchmark Model.

References

1) R. G. Sanchez, *et al.*, "Criticality of a ^{237}Np Sphere," Proc. 7th Int. Conf. on Nuclear Criticality Safety, ICNC 2003, Tokai-mura, Japan, Oct. 20-24, 2004 (2004).
2) D. Loaiza and R. Sanchez, "Analysis on the ^{237}Np Sphere Surrounded by ^{235}U Shells Experiment," Proc. 7th Int. Conf. on Nuclear Criticality Safety, ICNC 2003, Tokai-mura, Japan, Oct. 20-24, 2004 (2004).
3) R. Sanchez, D. Loaiza, and R. Kimpland "Criticality of a Neptunium-237 Sphere," *Trans. Am. Nucl. Soc.*, **88**, 88 (June 2003).
4) D. Loaiza, "Neptunium-237 Sphere Reflected by Hemispherical Shells of Highly Enriched Uranium," SPEC-MET-FAST-008, *International Handbook of Evaluated Criticality Safety Benchmark Experiments*, NEA/NSC/DOC(95)03 (rev.), OECD-NEA (September 2003).
5) *Ibid*., Appendix C.
6) X-5 Monte Carlo Team, "MCNP — A General Monte Carlo N-Particle Transport Code, Version 5, Volume I: Overview and Theory," LA-UR-03-1987, Los Alamos National Laboratory (April 2003).
7) Stephanie C. Frankle, Robert C. Reedy, and Phillip G. Young, "ACTI: An MCNP Data Library for Prompt Gamma-Ray Spectroscopy," Proc. 12th Biennial Topl. Mtg. Radiation Protection and Shielding Div., Santa Fe, New Mexico, April 14-18, 2002 (2002).
8) Joann M. Campbell, Stephanie C. Frankle, and Robert C. Little, "ENDF66: A Continuous-Energy Neutron Data Library for MCNP4C," Proc. 12th Biennial Topl. Mtg. Radiation Protection and Shielding Div., Santa Fe, New Mexico, April 14-18, 2002 (2002).
9) P. F. Rose, Ed., "ENDF-201, ENDF/B-VI Summary Documentation," BNL-NCS-17541, 4th Edition, Brookhaven National Laboratory (October 1991).
10) Personal communication, Yevgeniy Rozhikhin, Institute of Physics and Power Engineering, August 2003.

Appendix

Specifications for the Simplified Benchmark Model

The simplified benchmark is a combination of spheres, hemispheres, and cylinders, as was shown in Fig. 2. The central neptunium sphere is surrounded by separate annuli of tungsten and nickel. The gaps between those layers have been homogenized with the outer layer that encloses them. The nickel cladding rests on the aluminum liner of the bottom HEU hemisphere, which was created by homogenizing the bottom hemishells with the gaps between them. Similarly, the upper hemishells have been homogenized with the gaps between them to create a single, homogeneous hemisphere. The aluminum liners have been retained, as has a simplified model of the aluminum mounting tube (hereafter referred to as the pedestal). The outer edge of the bottom HEU hemisphere rests on the upper portion of the pedestal, whose inner edge fits snugly against it. The two HEU hemispheres are separated by a thin, cylindrical aluminum spacer, which produces a gap between the nickel cladding of the sphere and the aluminum liner of the upper HEU sphere. A cylindrical ring of aluminum encircles the spheres and hemispheres. That ring is displaced slightly downward relative to the center of the neptunium sphere.

A.1 Dimensions

Dimensions for the spheres and hemispheres are given in Table A-1, and those for the cylinders are given in Table A-2. The position of the cylindrical aluminum ring is such that its top is 1.5875 cm above the center of the neptunium sphere, and its bottom is 2.2225 cm below it.

A.2 Densities

The compositions of each of the materials in the final model are given in Tables A-3 through A-7. The chemical composition of the two aluminum liners in Table A-6 is identical, but the lower liner has been homogenized with a larger void region than has the upper. Consequently, the density of the homogenized lower liner is only 0.91753 times that of the upper one.

Table A-1 Radii of Spheres and Hemispheres.

Region	Inner Radius (cm)	Outer Radius (cm)
Neptunium Sphere	—	4.14909
Tungsten Cladding	4.14909	4.42722
Nickel Cladding	4.42722	4.81838
Lower Aluminum Liner	4.81838	5.01700
Lower HEU Hemisphere	5.01700	10.00000
Upper Aluminum Liner	4.83108	5.01300
Upper HEU Hemisphere	5.01300	9.66800

Table A-2 Dimensions of Cylinders.

Region	Inner Radius (cm)	Outer Radius (cm)	Height (cm)
Aluminum Shim	5.08000	10.00000	0.31750
Aluminum Ring	10.47750	16.51000	3.81000
Upper Portion of Pedestal	5.08000	7.62000	2.54000
Lower Portion of Pedestal	—	7.62000	4.76250

Table A-3 Composition of the Neptunium Sphere.

Isotope	Number Density (atoms/b-cm)
^{233}U	1.8577×10^{-6}
^{234}U	2.9633×10^{-7}
^{235}U	1.4074×10^{-5}
^{236}U	7.8349×10^{-8}
^{238}U	1.5626×10^{-6}
^{237}Np	5.0926×10^{-2}
^{238}Pu	8.2304×10^{-7}
^{239}Pu	1.6271×10^{-5}
^{240}Pu	1.1619×10^{-6}
^{241}Pu	3.1166×10^{-8}
^{242}Pu	1.6032×10^{-7}
^{241}Am	3.3375×10^{-7}
^{243}Am	9.1575×10^{-5}

Table A-4 Composition of the Homogenized Tungsten Cladding.

Isotope or Element	Number Density (atoms/b-cm)
Iron	3.4491×10^{-3}
Nickel	3.2820×10^{-3}
^{182}W	1.4057×10^{-2}
^{183}W	7.5931×10^{-3}
^{184}W	1.6254×10^{-2}
^{186}W	1.5079×10^{-2}

Table A-5 Composition of the Homogenized Nickel Cladding.

Element	Number Density (atoms/b-cm)
Nickel	8.5344×10^{-2}

Table A-6 Composition of Al-6061-T6 for the Homogenized Liners.

Isotope or Element	Number Density (atoms/b-cm)	
	Upper Liner	Lower Liner
Magnesium	7.1200×10^{-4}	6.5328×10^{-4}
^{27}Al	5.5475×10^{-2}	5.0900×10^{-2}
Silicon	3.2862×10^{-4}	3.0152×10^{-4}
Titanium	2.4102×10^{-5}	2.2114×10^{-5}
Chromium	5.7689×10^{-5}	5.2931×10^{-5}
^{55}Mn	2.1000×10^{-5}	1.9268×10^{-5}
Iron	9.6403×10^{-5}	8.8452×10^{-5}
Copper	6.6568×10^{-5}	6.1078×10^{-5}

Table A-7 Composition of the HEU Hemispheres.

Isotope	Number Density (atoms/b-cm)
^{234}U	4.7468×10^{-4}
^{235}U	4.3169×10^{-2}
^{236}U	2.1687×10^{-4}
^{238}U	2.4478×10^{-3}